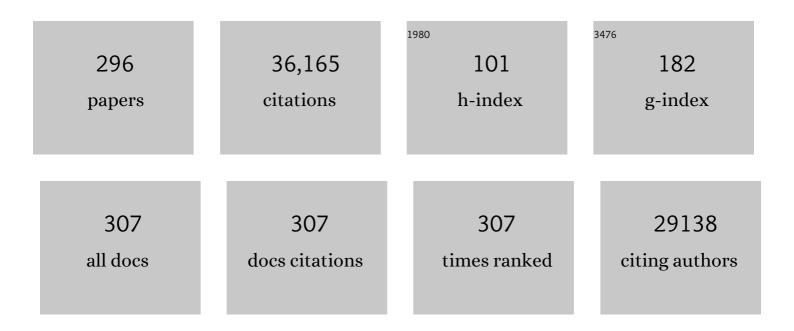
List of Publications by Year in descending order

Source: https://exaly.com/author-pdf/3476628/publications.pdf Version: 2024-02-01



RELLONG

#	Article	IF	CITATIONS
1	Flexible solid-state supercapacitors: design, fabrication and applications. Energy and Environmental Science, 2014, 7, 2160.	15.6	1,156
2	Flexible Energy‧torage Devices: Design Consideration and Recent Progress. Advanced Materials, 2014, 26, 4763-4782.	11.1	1,153
3	Dendriteâ€Free Zinc Deposition Induced by Multifunctional CNT Frameworks for Stable Flexible Znâ€ion Batteries. Advanced Materials, 2019, 31, e1903675.	11.1	780
4	Polyaniline and Polypyrrole Pseudocapacitor Electrodes with Excellent Cycling Stability. Nano Letters, 2014, 14, 2522-2527.	4.5	688
5	Solidâ€ S tate Supercapacitor Based on Activated Carbon Cloths Exhibits Excellent Rate Capability. Advanced Materials, 2014, 26, 2676-2682.	11.1	660
6	WO _{3–x} @Au@MnO ₂ Core–Shell Nanowires on Carbon Fabric for Highâ€Performance Flexible Supercapacitors. Advanced Materials, 2012, 24, 938-944.	11.1	641
7	Stabilized TiN Nanowire Arrays for High-Performance and Flexible Supercapacitors. Nano Letters, 2012, 12, 5376-5381.	4.5	627
8	FeOOH/Co/FeOOH Hybrid Nanotube Arrays as Highâ€Performance Electrocatalysts for the Oxygen Evolution Reaction. Angewandte Chemie - International Edition, 2016, 55, 3694-3698.	7.2	611
9	Design and Synthesis of FeOOH/CeO ₂ Heterolayered Nanotube Electrocatalysts for the Oxygen Evolution Reaction. Advanced Materials, 2016, 28, 4698-4703.	11.1	592
10	Achieving Ultrahigh Energy Density and Long Durability in a Flexible Rechargeable Quasiâ€6olidâ€6tate Zn–MnO ₂ Battery. Advanced Materials, 2017, 29, 1700274.	11.1	572
11	Efficient Hydrogen Evolution on Cu Nanodots-Decorated Ni ₃ S ₂ Nanotubes by Optimizing Atomic Hydrogen Adsorption and Desorption. Journal of the American Chemical Society, 2018, 140, 610-617.	6.6	563
12	A review of carbon materials and their composites with alloy metals for sodium ion battery anodes. Carbon, 2016, 98, 162-178.	5.4	527
13	Hierarchical NiCo ₂ O ₄ nanosheets@hollow microrod arrays for high-performance asymmetric supercapacitors. Journal of Materials Chemistry A, 2014, 2, 4706-4713.	5.2	488
14	Facile synthesis of large-area manganese oxide nanorod arrays as a high-performance electrochemical supercapacitor. Energy and Environmental Science, 2011, 4, 2915.	15.6	479
15	Activating CoOOH Porous Nanosheet Arrays by Partial Iron Substitution for Efficient Oxygen Evolution Reaction. Angewandte Chemie - International Edition, 2018, 57, 2672-2676.	7.2	474
16	Co3O4/Ni(OH)2 composite mesoporous nanosheet networks as a promising electrode for supercapacitor applications. Journal of Materials Chemistry, 2012, 22, 5656.	6.7	471
17	Nitrogenâ€Doped Co ₃ O ₄ Mesoporous Nanowire Arrays as an Additiveâ€Free Airâ€Cathode for Flexible Solidâ€State Zinc–Air Batteries. Advanced Materials, 2017, 29, 1602868.	11.1	428
18	Pt-like Hydrogen Evolution Electrocatalysis on PANI/CoP Hybrid Nanowires by Weakening the Shackles of Hydrogen lons on the Surfaces of Catalysts. Journal of the American Chemical Society, 2018, 140, 5118-5126.	6.6	425

#	Article	IF	CITATIONS
19	Advanced Tiâ€Doped Fe ₂ O ₃ @PEDOT Core/Shell Anode for Highâ€Energy Asymmetric Supercapacitors. Advanced Energy Materials, 2015, 5, 1402176.	10.2	416
20	Flexible Znâ€lon Batteries: Recent Progresses and Challenges. Small, 2019, 15, e1804760.	5.2	412
21	WO _{3â^'<i>x</i>} /MoO _{3â^'<i>x</i>} Core/Shell Nanowires on Carbon Fabric as an Anode for Allâ€6olidâ€6tate Asymmetric Supercapacitors. Advanced Energy Materials, 2012, 2, 1328-1332.	10.2	401
22	Recent advances in metal nitrides as high-performance electrode materials for energy storage devices. Journal of Materials Chemistry A, 2015, 3, 1364-1387.	5.2	396
23	A Novel Exfoliation Strategy to Significantly Boost the Energy Storage Capability of Commercial Carbon Cloth. Advanced Materials, 2015, 27, 3572-3578.	11.1	384
24	Oxygen Vacancy Induced Bismuth Oxyiodide with Remarkably Increased Visible-Light Absorption and Superior Photocatalytic Performance. ACS Applied Materials & Interfaces, 2014, 6, 22920-22927.	4.0	370
25	α-Fe ₂ O ₃ @PANI Core–Shell Nanowire Arrays as Negative Electrodes for Asymmetric Supercapacitors. ACS Applied Materials & Interfaces, 2015, 7, 14843-14850.	4.0	369
26	Porous Microrod Arrays Constructed by Carbon onfined NiCo@NiCoO ₂ Core@Shell Nanoparticles as Efficient Electrocatalysts for Oxygen Evolution. Advanced Materials, 2018, 30, e1705442.	11.1	366
27	Ironâ€Based Supercapacitor Electrodes: Advances and Challenges. Advanced Energy Materials, 2016, 6, 1601053.	10.2	358
28	Updates on the development of nanostructured transition metal nitrides for electrochemical energy storage and water splitting. Materials Today, 2017, 20, 425-451.	8.3	339
29	Spongeâ€Like Piezoelectric Polymer Films for Scalable and Integratable Nanogenerators and Selfâ€Powered Electronic Systems. Advanced Energy Materials, 2014, 4, 1301624.	10.2	326
30	An Ultrastable and Highâ€Performance Flexible Fiberâ€Shaped Ni–Zn Battery based on a Ni–NiO Heterostructured Nanosheet Cathode. Advanced Materials, 2017, 29, 1702698.	11.1	314
31	Boosting Znâ€lon Energy Storage Capability of Hierarchically Porous Carbon by Promoting Chemical Adsorption. Advanced Materials, 2019, 31, e1904948.	11.1	304
32	Efficient Hydrogen Evolution Electrocatalysis Using Cobalt Nanotubes Decorated with Titanium Dioxide Nanodots. Angewandte Chemie - International Edition, 2017, 56, 2960-2964.	7.2	303
33	Co(OH) ₂ @PANI Hybrid Nanosheets with 3D Networks as Highâ€Performance Electrocatalysts for Hydrogen Evolution Reaction. Advanced Materials, 2015, 27, 7051-7057.	11.1	294
34	Boosting the Energy Density of Carbonâ€Based Aqueous Supercapacitors by Optimizing the Surface Charge. Angewandte Chemie - International Edition, 2017, 56, 5454-5459.	7.2	292
35	Scalable self-growth of Ni@NiO core-shell electrode with ultrahigh capacitance and super-long cyclic stability for supercapacitors. NPG Asia Materials, 2014, 6, e129-e129.	3.8	284
36	High-performance flexible quasi-solid-state Zn–MnO ₂ battery based on MnO ₂ nanorod arrays coated 3D porous nitrogen-doped carbon cloth. Journal of Materials Chemistry A, 2017, 5, 14838-14846.	5.2	273

#	Article	IF	CITATIONS
37	Single-crystal ZnO nanorod/amorphous and nanoporous metal oxide shell composites: Controllable electrochemical synthesis and enhanced supercapacitor performances. Energy and Environmental Science, 2011, 4, 1288.	15.6	271
38	Bifunctional catalytic material: An ultrastable and high-performance surface defect CeO2 nanosheets for formaldehyde thermal oxidation and photocatalytic oxidation. Applied Catalysis B: Environmental, 2016, 181, 779-787.	10.8	268
39	Nitrogen treatment generates tunable nanohybridization of Ni5P4 nanosheets with nickel hydr(oxy)oxides for efficient hydrogen production in alkaline, seawater and acidic media. Applied Catalysis B: Environmental, 2019, 251, 181-194.	10.8	260
40	Multiscale Pore Network Boosts Capacitance of Carbon Electrodes for Ultrafast Charging. Nano Letters, 2017, 17, 3097-3104.	4.5	251
41	Dualâ€Doped Molybdenum Trioxide Nanowires: A Bifunctional Anode for Fiberâ€Shaped Asymmetric Supercapacitors and Microbial Fuel Cells. Angewandte Chemie - International Edition, 2016, 55, 6762-6766.	7.2	230
42	Electrochemical Synthesis of Polyaniline Nanobelts with Predominant Electrochemical Performances. Macromolecules, 2010, 43, 2178-2183.	2.2	223
43	Heterojunction Architecture of Nâ€Doped WO ₃ Nanobundles with Ce ₂ S ₃ Nanodots Hybridized on a Carbon Textile Enables a Highly Efficient Flexible Photocatalyst. Advanced Functional Materials, 2019, 29, 1903490.	7.8	223
44	Flexible Ultrafast Aqueous Rechargeable Ni//Bi Battery Based on Highly Durable Singleâ€Crystalline Bismuth Nanostructured Anode. Advanced Materials, 2016, 28, 9188-9195.	11.1	220
45	Charge Relays via Dual Carbonâ€Actions on Nanostructured BiVO ₄ for High Performance Photoelectrochemical Water Splitting. Advanced Functional Materials, 2022, 32, .	7.8	219
46	Achieving high gravimetric energy density for flexible lithium-ion batteries facilitated by core–double-shell electrodes. Energy and Environmental Science, 2018, 11, 1859-1869.	15.6	216
47	Silica–Polypyrrole Hybrids as Highâ€Performance Metalâ€Free Electrocatalysts for the Hydrogen Evolution Reaction in Neutral Media. Angewandte Chemie - International Edition, 2017, 56, 8120-8124.	7.2	214
48	Controllable synthesis of porous nickel–cobalt oxide nanosheets for supercapacitors. Journal of Materials Chemistry, 2012, 22, 13357.	6.7	207
49	Morphology and Doping Engineering of Sn-Doped Hematite Nanowire Photoanodes. Nano Letters, 2017, 17, 2490-2495.	4.5	204
50	Three-dimensional nickel nitride (Ni ₃ N) nanosheets: free standing and flexible electrodes for lithium ion batteries and supercapacitors. Journal of Materials Chemistry A, 2016, 4, 9844-9849.	5.2	203
51	Valenceâ€Optimized Vanadium Oxide Supercapacitor Electrodes Exhibit Ultrahigh Capacitance and Superâ€Long Cyclic Durability of 100 000 Cycles. Advanced Functional Materials, 2015, 25, 3534-3540.	7.8	200
52	Asymmetric Paper Supercapacitor Based on Amorphous Porous Mn ₃ O ₄ Negative Electrode and Ni(OH) ₂ Positive Electrode: A Novel and High-Performance Flexible Electrochemical Energy Storage Device. ACS Applied Materials & Interfaces, 2015, 7, 11444-11451.	4.0	198
53	A review of the development of full cell lithium-ion batteries: The impact of nanostructured anode materials. Nano Research, 2016, 9, 2823-2851.	5.8	198
54	A monolithic metal-free electrocatalyst for oxygen evolution reaction and overall water splitting. Energy and Environmental Science, 2016, 9, 3411-3416.	15.6	197

#	Article	IF	CITATIONS
55	A Facile Activation Strategy for an MOF-Derived Metal-Free Oxygen Reduction Reaction Catalyst: Direct Access to Optimized Pore Structure and Nitrogen Species. ACS Catalysis, 2017, 7, 6082-6088.	5.5	188
56	High power density nitridated hematite (α-Fe2O3) nanorods as anode for high-performance flexible lithium ion batteries. Journal of Power Sources, 2016, 308, 7-17.	4.0	182
57	Binder-free Fe2N nanoparticles on carbon textile with high power density as novel anode for high-performance flexible lithium ion batteries. Nano Energy, 2015, 11, 348-355.	8.2	180
58	ZnO@MoO3 core/shell nanocables: facile electrochemical synthesis and enhanced supercapacitor performances. Journal of Materials Chemistry, 2011, 21, 4217.	6.7	178
59	Holey Tungsten Oxynitride Nanowires: Novel Anodes Efficiently Integrate Microbial Chemical Energy Conversion and Electrochemical Energy Storage. Advanced Materials, 2015, 27, 3085-3091.	11.1	177
60	Costâ€Effective Alkaline Water Electrolysis Based on Nitrogen―and Phosphorusâ€Doped Selfâ€Supportive Electrocatalysts. Advanced Materials, 2017, 29, 1702095.	11.1	175
61	Quantitative Detection of Photothermal and Photoelectrocatalytic Effects Induced by SPR from Au@Pt Nanoparticles. Angewandte Chemie - International Edition, 2015, 54, 11462-11466.	7.2	169
62	All-flexible lithium ion battery based on thermally-etched porous carbon cloth anode and cathode. Nano Energy, 2016, 26, 446-455.	8.2	167
63	Engineering Thin MoS ₂ Nanosheets on TiN Nanorods: Advanced Electrochemical Capacitor Electrode and Hydrogen Evolution Electrocatalyst. ACS Energy Letters, 2017, 2, 1862-1868.	8.8	167
64	Co-based MOF-derived Co/CoN/Co2P ternary composite embedded in N- and P-doped carbon as bifunctional nanocatalysts for efficient overall water splitting. International Journal of Hydrogen Energy, 2019, 44, 11402-11410.	3.8	167
65	Enhancing the Capacitive Storage Performance of Carbon Fiber Textile by Surface and Structural Modulation for Advanced Flexible Asymmetric Supercapacitors. Advanced Functional Materials, 2019, 29, 1806329.	7.8	167
66	A novel highly luminescent LnMOF film: a convenient sensor for Hg2+ detecting. Journal of Materials Chemistry A, 2013, 1, 11312.	5.2	166
67	Cerium-based hybrid nanorods for synergetic photo-thermocatalytic degradation of organic pollutants. Journal of Materials Chemistry A, 2018, 6, 24740-24747.	5.2	164
68	Solar driven hydrogen releasing from urea and human urine. Energy and Environmental Science, 2012, 5, 8215.	15.6	160
69	Carbon Quantum Dot Surface-Engineered VO ₂ Interwoven Nanowires: A Flexible Cathode Material for Lithium and Sodium Ion Batteries. ACS Applied Materials & Interfaces, 2016, 8, 9733-9744.	4.0	158
70	Efficient Charges Separation Using Advanced BiOI-Based Hollow Spheres Decorated with Palladium and Manganese Dioxide Nanoparticles. ACS Sustainable Chemistry and Engineering, 2018, 6, 2751-2757.	3.2	157
71	Building Threeâ€Ðimensional Graphene Frameworks for Energy Storage and Catalysis. Advanced Functional Materials, 2015, 25, 324-330.	7.8	156
72	Polyaniline nanotube arrays as high-performance flexible electrodes for electrochemical energy storage devices. Journal of Materials Chemistry, 2012, 22, 2401.	6.7	149

#	Article	IF	CITATIONS
73	Water Surface Assisted Synthesis of Largeâ€6cale Carbon Nanotube Film for Highâ€Performance and Stretchable Supercapacitors. Advanced Materials, 2014, 26, 4724-4729.	11.1	148
74	Ni ₂ P–CoP hybrid nanosheet arrays supported on carbon cloth as an efficient flexible cathode for hydrogen evolution. Journal of Materials Chemistry A, 2016, 4, 16992-16999.	5.2	148
75	Recent Smart Methods for Achieving Highâ€Energy Asymmetric Supercapacitors. Small Methods, 2018, 2, 1700230.	4.6	147
76	A Confinement Strategy for Stabilizing ZIFâ€Derived Bifunctional Catalysts as a Benchmark Cathode of Flexible Allâ€Solidâ€State Zinc–Air Batteries. Advanced Materials, 2018, 30, e1805268.	11.1	147
77	Ostwald Ripening Improves Rate Capability of High Mass Loading Manganese Oxide for Supercapacitors. ACS Energy Letters, 2017, 2, 1752-1759.	8.8	146
78	Facile synthesis of titanium nitride nanowires on carbon fabric for flexible and high-rate lithium ion batteries. Journal of Materials Chemistry A, 2014, 2, 10825-10829.	5.2	145
79	Enhanced BiVO ₄ Photoanode Photoelectrochemical Performance via Borate Treatment and a NiFeOx Cocatalyst. ACS Sustainable Chemistry and Engineering, 2021, 9, 8306-8314.	3.2	144
80	Enhanced Catalytic Activity and Stability of Pt/CeO ₂ /PANI Hybrid Hollow Nanorod Arrays for Methanol Electro-oxidation. ACS Catalysis, 2016, 6, 5198-5206.	5.5	140
81	In Situ Activation of 3D Porous Bi/Carbon Architectures: Toward Highâ€Energy and Stable Nickel–Bismuth Batteries. Advanced Materials, 2018, 30, e1707290.	11.1	139
82	Three dimensional architectures: design, assembly and application in electrochemical capacitors. Journal of Materials Chemistry A, 2015, 3, 15792-15823.	5.2	135
83	Ceria and ceria-based nanostructured materials for photoenergy applications. Nano Energy, 2017, 34, 313-337.	8.2	134
84	Acid Treatment Enables Suppression of Electron–Hole Recombination in Hematite for Photoelectrochemical Water Splitting. Angewandte Chemie - International Edition, 2016, 55, 3403-3407.	7.2	132
85	Oxygen Defects in Promoting the Electrochemical Performance of Metal Oxides for Supercapacitors: Recent Advances and Challenges. Small Methods, 2020, 4, 1900823.	4.6	129
86	FeOOH/Co/FeOOH Hybrid Nanotube Arrays as Highâ€Performance Electrocatalysts for the Oxygen Evolution Reaction. Angewandte Chemie, 2016, 128, 3758-3762.	1.6	128
87	Phase Boundary Derived Pseudocapacitance Enhanced Nickelâ€Based Composites for Electrochemical Energy Storage Devices. Advanced Energy Materials, 2018, 8, 1701681.	10.2	124
88	Nickel@Nickel Oxide Core–Shell Electrode with Significantly Boosted Reactivity for Ultrahighâ€Energy and Stable Aqueous Ni–Zn Battery. Advanced Functional Materials, 2018, 28, 1802157.	7.8	123
89	Redox cycles promoting photocatalytic hydrogen evolution of CeO2 nanorods. Journal of Materials Chemistry, 2011, 21, 5569.	6.7	120
90	Efficient Hydrogen Evolution Activity and Overall Water Splitting of Metallic Co ₄ N Nanowires through Tunable d-Orbitals with Ultrafast Incorporation of FeOOH. ACS Applied Materials & Interfaces, 2019, 11, 5152-5158.	4.0	120

#	Article	IF	CITATIONS
91	An Electrochemical Capacitor with Applicable Energy Density of 7.4 Wh/kg at Average Power Density of 3000 W/kg. Nano Letters, 2015, 15, 3189-3194.	4.5	118
92	Vanadium Nitride Nanowire Supported SnS ₂ Nanosheets with High Reversible Capacity as Anode Material for Lithium Ion Batteries. ACS Applied Materials & Interfaces, 2015, 7, 23205-23215.	4.0	115
93	Nitrogen and Phosphorus Codoped Vertical Graphene/Carbon Cloth as a Binderâ€Free Anode for Flexible Advanced Potassium Ion Full Batteries. Small, 2019, 15, e1901285.	5.2	115
94	Titanium dioxide@titanium nitride nanowires on carbon cloth with remarkable rate capability for flexible lithium-ion batteries. Journal of Power Sources, 2014, 272, 946-953.	4.0	114
95	An electrochemical method to enhance the performance of metal oxides for photoelectrochemical water oxidation. Journal of Materials Chemistry A, 2016, 4, 2849-2855.	5.2	114
96	Large-Scale Electric-Field Confined Silicon with Optimized Charge-Transfer Kinetics and Structural Stability for High-Rate Lithium-Ion Batteries. ACS Nano, 2020, 14, 7066-7076.	7.3	114
97	The roles of defect states in photoelectric and photocatalytic processes for Zn _x Cd _{1â^x} S. Energy and Environmental Science, 2011, 4, 466-470.	15.6	112
98	Improving the photoelectrochemical and photocatalytic performance of CdO nanorods with CdS decoration. CrystEngComm, 2013, 15, 4212.	1.3	110
99	Oxygen Defect Modulated Titanium Niobium Oxide on Graphene Arrays: An Openâ€Door for Highâ€Performance 1.4 V Symmetric Supercapacitor in Acidic Aqueous Electrolyte. Advanced Functional Materials, 2018, 28, 1805618.	7.8	110
100	Rational design of atomically dispersed nickel active sites in β-Mo ₂ C for the hydrogen evolution reaction at all pH values. Chemical Communications, 2018, 54, 9901-9904.	2.2	110
101	Enhanced Efficiency of Electron–Hole Separation in Bi ₂ O ₂ CO ₃ for Photocatalysis via Acid Treatment. ChemCatChem, 2018, 10, 1982-1987.	1.8	104
102	Emerging porous materials in confined spaces: from chromatographic applications to flow chemistry. Chemical Society Reviews, 2019, 48, 2566-2595.	18.7	103
103	Sulphur-doped Co ₃ O ₄ nanowires as an advanced negative electrode for high-energy asymmetric supercapacitors. Journal of Materials Chemistry A, 2016, 4, 10779-10785.	5.2	101
104	Remarkable photoelectrochemical performance of carbon dots sensitized TiO ₂ under visible light irradiation. Journal of Materials Chemistry A, 2014, 2, 16365-16368.	5.2	100
105	Oxygen vacancy–based metal oxides photoanodes in photoelectrochemical water splitting. Materials Today Sustainability, 2022, 18, 100118.	1.9	100
106	3D CNTs Networks Enable MnO ₂ Cathodes with High Capacity and Superior Rate Capability for Flexible Rechargeable Zn–MnO ₂ Batteries. Small Methods, 2019, 3, 1900525.	4.6	99
107	Polypyrrole-encapsulated amorphous Bi ₂ S ₃ hollow sphere for long life sodium ion batteries and lithium–sulfur batteries. Journal of Materials Chemistry A, 2019, 7, 11370-11378.	5.2	99
108	Pt Nanorods Aggregates with Enhanced Electrocatalytic Activity toward Methanol Oxidation. Journal of Physical Chemistry C, 2010, 114, 19175-19181.	1.5	98

#	Article	IF	CITATIONS
109	Engineering of Mesoscale Pores in Balancing Mass Loading and Rate Capability of Hematite Films for Electrochemical Capacitors. Advanced Energy Materials, 2018, 8, 1801784.	10.2	97
110	Activated carbon fiber paper with exceptional capacitive performance as a robust electrode for supercapacitors. Journal of Materials Chemistry A, 2016, 4, 5828-5833.	5.2	95
111	Defect Engineering of Bismuth Oxyiodide by IO ₃ [–] Doping for Increasing Charge Transport in Photocatalysis. ACS Applied Materials & Interfaces, 2016, 8, 27859-27867.	4.0	93
112	Dual Doping Induced Interfacial Engineering of Fe ₂ N/Fe ₃ N Hybrids with Favorable dâ€Band towards Efficient Overall Water Splitting. ChemCatChem, 2019, 11, 6051-6060.	1.8	92
113	Intermediates Adsorption Engineering of CO ₂ Electroreduction Reaction in Highly Selective Heterostructure Cuâ€Based Electrocatalysts for CO Production. Advanced Energy Materials, 2019, 9, 1901396.	10.2	92
114	Asymmetric supercapacitors with high energy density based on helical hierarchical porous Na _x MnO ₂ and MoO ₂ . Chemical Science, 2016, 7, 510-517.	3.7	89
115	Binder-free WS ₂ nanosheets with enhanced crystallinity as a stable negative electrode for flexible asymmetric supercapacitors. Journal of Materials Chemistry A, 2017, 5, 21460-21466.	5.2	89
116	Synthesis, crystal structures and properties of six cubane-like transition metal complexes of di-2-pyridyl ketone in gem-diol form. Dalton Transactions RSC, 2002, , 1727-1734.	2.3	88
117	Tunable Wavelength Enhanced Photoelectrochemical Cells from Surface Plasmon Resonance. Journal of the American Chemical Society, 2016, 138, 16204-16207.	6.6	87
118	Porous CeO2 nanowires/nanowire arrays: electrochemical synthesis and application in water treatment. Journal of Materials Chemistry, 2010, 20, 7118.	6.7	86
119	Designing Carbon Based Supercapacitors with High Energy Density: A Summary of Recent Progress. Chemistry - A European Journal, 2018, 24, 7312-7329.	1.7	86
120	A Flexible Microsupercapacitor with Integral Photocatalytic Fuel Cell for Self-Charging. ACS Nano, 2019, 13, 8246-8255.	7.3	86
121	Enhanced photoactivity and stability of carbon and nitrogen co-treated ZnO nanorod arrays for photoelectrochemical water splitting. Journal of Materials Chemistry, 2012, 22, 14272.	6.7	85
122	A review of negative electrode materials for electrochemical supercapacitors. Science China Technological Sciences, 2015, 58, 1799-1808.	2.0	84
123	Recent advances and challenges of stretchable supercapacitors based on carbon materials. Science China Materials, 2016, 59, 475-494.	3.5	83
124	Enhancing the Photocatalytic Performance of BiOCl <i>_x</i> l _{1â^'<i>x</i>} by Introducing Surface Disorders and Bi Nanoparticles as Cocatalyst. Advanced Materials Interfaces, 2015, 2, 1500249.	1.9	82
125	Zipping Up NiFe(OH) _{<i>x</i>} -Encapsulated Hematite To Achieve an Ultralow Turn-On Potential for Water Oxidation. ACS Energy Letters, 2019, 4, 1983-1990.	8.8	82
126	Alkali-modified non-precious metal 3D-NiCo ₂ O ₄ nanosheets for efficient formaldehyde oxidation at low temperature. Journal of Materials Chemistry A, 2016, 4, 3648-3654.	5.2	81

#	Article	IF	CITATIONS
127	Ultrathin Bi ₂ MoO ₆ Nanosheets for Photocatalysis: Performance Enhancement by Atomic Interfacial Engineering. ChemistrySelect, 2018, 3, 7423-7428.	0.7	81
128	Monodisperse CeO2/CdS heterostructured spheres: one-pot synthesis and enhanced photocatalytic hydrogen activity. RSC Advances, 2011, 1, 1207.	1.7	80
129	Controllable Electrochemical Synthesis of Hierarchical ZnO Nanostructures on FTO Glass. Journal of Physical Chemistry C, 2009, 113, 13574-13582.	1.5	79
130	Fe ₃ O ₄ /reduced graphene oxide with enhanced electrochemical performance towards lithium storage. Journal of Materials Chemistry A, 2014, 2, 7214-7220.	5.2	79
131	Co(II) _{1–<i>x</i>} Co(0) _{<i>x</i>/3} Mn(III) _{2<i>x</i>/3} S Nanoparticles Supported on B/N-Codoped Mesoporous Nanocarbon as a Bifunctional Electrocatalyst of Oxygen Reduction/Evolution for High-Performance Zinc-Air Batteries. ACS Applied Materials & amp; Interfaces, 2016. 8. 13348-13359.	4.0	77
132	Chemically Lithiated TiO ₂ Heterostructured Nanosheet Anode with Excellent Rate Capability and Long Cycle Life for High-Performance Lithium-Ion Batteries. ACS Applied Materials & Interfaces, 2015, 7, 25991-26003.	4.0	76
133	Controllable synthesis of hierarchical ZnO nanodisks for highly photocatalytic activity. CrystEngComm, 2012, 14, 1850.	1.3	75
134	A modified molecular framework derived highly efficient Mn–Co–carbon cathode for a flexible Zn–air battery. Chemical Communications, 2017, 53, 11596-11599.	2.2	75
135	Ni@NiO core–shell nanoparticle tube arrays with enhanced supercapacitor performance. Journal of Materials Chemistry A, 2015, 3, 6432-6439.	5.2	73
136	Hydrogen production from solar driven glucose oxidation over Ni(OH)2 functionalized electroreduced-TiO2 nanowire arrays. Green Chemistry, 2013, 15, 2434.	4.6	72
137	Glucose-Induced Formation of Oxygen Vacancy and Bi-Metal Comodified Bi ₅ O ₇ Br Nanotubes for Efficient Performance Photocatalysis. ACS Sustainable Chemistry and Engineering, 2019, 7, 5784-5791.	3.2	72
138	Dualâ€Doped Molybdenum Trioxide Nanowires: A Bifunctional Anode for Fiberâ€Shaped Asymmetric Supercapacitors and Microbial Fuel Cells. Angewandte Chemie, 2016, 128, 6874-6878.	1.6	70
139	Encapsulated Vanadiumâ€Based Hybrids in Amorphous Nâ€Doped Carbon Matrix as Anode Materials for Lithiumâ€lon Batteries. Small, 2017, 13, 1702081.	5.2	70
140	Flexible symmetrical planar supercapacitors based on multi-layered MnO ₂ /Ni/graphite/paper electrodes with high-efficient electrochemical energy storage. Journal of Materials Chemistry A, 2014, 2, 2985-2992.	5.2	69
141	Ultrathin MXene "bridge―to accelerate charge transfer in ultrathin metal-free 0D/2D black phosphorus/g-C3N4 heterojunction toward photocatalytic hydrogen production. Journal of Colloid and Interface Science, 2021, 584, 474-483.	5.0	69
142	Sulfurization of FeOOH nanorods on a carbon cloth and their conversion into Fe ₂ O ₃ /Fe ₃ O ₄ –S coreâ^'shell nanorods for lithium storage. Chemical Communications, 2015, 51, 13016-13019.	2.2	68
143	Design of a 1D/2D C3N4/rGO composite as an anode material for stable and effective potassium storage. Energy Storage Materials, 2020, 25, 495-501.	9.5	68
144	High-performance supercapacitors based on MnO ₂ tube-in-tube arrays. Journal of Materials Chemistry A, 2015, 3, 16560-16566.	5.2	67

#	Article	IF	CITATIONS
145	Enhanced metallicity boosts hydrogen evolution capability of dual-bimetallic Ni–Fe nitride nanoparticles. Materials Today Physics, 2020, 15, 100267.	2.9	67
146	Boosting the Oxygen Evolution Reaction Activity of NiFe ₂ O ₄ Nanosheets by Phosphate Ion Functionalization. ACS Omega, 2019, 4, 3493-3499.	1.6	66
147	Engineering the Band-Edge of Fe ₂ O ₃ /ZnO Nanoplates via Separate Dual Cation Incorporation for Efficient Photocatalytic Performance. Industrial & Engineering Chemistry Research, 2020, 59, 18865-18872.	1.8	66
148	Facile electrochemical synthesis of CeO ₂ hierarchical nanorods and nanowires with excellent photocatalytic activities. New Journal of Chemistry, 2014, 38, 2581-2586.	1.4	64
149	Low concentration nitric acid facilitate rapid electron–hole separation in vacancy-rich bismuth oxyiodide for photo-thermo-synergistic oxidation of formaldehyde. Applied Catalysis B: Environmental, 2017, 218, 700-708.	10.8	64
150	Freeing the Polarons to Facilitate Charge Transport in BiVO ₄ from Oxygen Vacancies with an Oxidative 2D Precursor. Angewandte Chemie - International Edition, 2019, 58, 19087-19095.	7.2	64
151	Engineering of Oxygen Vacancy and Electricâ€Field Effect by Encapsulating Lithium Titanate in Reduced Graphene Oxide for Superior Lithium Ion Storage. Small Methods, 2019, 3, 1900185.	4.6	64
152	Co ₃ O ₄ @Cuâ€Based Conductive Metal–Organic Framework Core–Shell Nanowire Electrocatalysts Enable Efficient Lowâ€Overallâ€Potential Water Splitting. Chemistry - A European Journal, 2019, 25, 6575-6583.	1.7	64
153	Surface engineering of carbon fiber paper for efficient capacitive energy storage. Journal of Materials Chemistry A, 2016, 4, 18639-18645.	5.2	63
154	Room-temperature ferromagnetism in hierarchically branched MoO ₃ nanostructures. CrystEngComm, 2012, 14, 1419-1424.	1.3	62
155	High-performance polypyrrole functionalized PtPd electrocatalysts based on PtPd/PPy/PtPd three-layered nanotube arrays for the electrooxidation of small organic molecules. NPG Asia Materials, 2013, 5, e69-e69.	3.8	62
156	CdS/CeOx heterostructured nanowires for photocatalytic hydrogen production. Journal of Materials Chemistry A, 2013, 1, 4190.	5.2	61
157	Pt–MoO ₃ –RGO ternary hybrid hollow nanorod arrays as high-performance catalysts for methanol electrooxidation. Journal of Materials Chemistry A, 2016, 4, 1923-1930.	5.2	60
158	Boosting the Energy Density of Carbonâ€Based Aqueous Supercapacitors by Optimizing the Surface Charge. Angewandte Chemie, 2017, 129, 5546-5551.	1.6	60
159	Vertically aligned In2O3 nanorods on FTO substrates for photoelectrochemical applications. Journal of Materials Chemistry, 2011, 21, 14685.	6.7	59
160	Photohole Induced Corrosion of Titanium Dioxide: Mechanism and Solutions. Nano Letters, 2015, 15, 7051-7057.	4.5	57
161	Interface charges redistribution enhanced monolithic etched copper foam-based Cu2O layer/TiO2 nanodots heterojunction with high hydrogen evolution electrocatalytic activity. Applied Catalysis B: Environmental, 2019, 243, 365-372.	10.8	56
162	Synergistic Performance between Visible-Light Photocatalysis and Thermocatalysis for VOCs Oxidation over Robust Ag/F-Codoped SrTiO ₃ . Industrial & Engineering Chemistry Research, 2018, 57, 12766-12773.	1.8	55

#	Article	IF	CITATIONS
163	Influence of ligand backbones and counter ions on structures of helical silver(I) complexes with di-Schiff bases derived from phthalaldehydes and diamine. Dalton Transactions RSC, 2000, , 4182-4186.	2.3	53
164	Facile hydrothermal synthesis of Bi2S3 spheres and CuS/Bi2S3 composites nanostructures with enhanced visible-light photocatalytic performances. CrystEngComm, 2012, 14, 8261.	1.3	52
165	High pseudocapacitance boosts the performance of monolithic porous carbon cloth/closely packed TiO ₂ nanodots as an anode of an all-flexible sodium-ion battery. Journal of Materials Chemistry A, 2019, 7, 2626-2635.	5.2	52
166	p-BiOI/n-SnS ₂ heterojunction flowerlike structure with enhanced visible-light photocatalytic performance. RSC Advances, 2015, 5, 15469-15478.	1.7	51
167	Solar-microbial hybrid device based on oxygen-deficient niobium pentoxide anodes for sustainable hydrogen production. Chemical Science, 2015, 6, 6799-6805.	3.7	51
168	Luminescent Lanthanide Complexes with Encapsulating Polybenzimidazole Tripodal Ligands. Inorganic Chemistry, 1999, 38, 1374-1375.	1.9	50
169	Efficient Photoelectrochemical Water Oxidation over Hydrogenâ€Reduced Nanoporous BiVO ₄ with Ni–B _i Electrocatalyst. ChemElectroChem, 2015, 2, 1385-1395.	1.7	50
170	In Situ Hydrothermally Grown TiO ₂ @C Core–Shell Nanowire Coating for Highly Sensitive Solid Phase Microextraction of Polycyclic Aromatic Hydrocarbons. ACS Applied Materials & Interfaces, 2017, 9, 1840-1846.	4.0	50
171	Activating CoOOH Porous Nanosheet Arrays by Partial Iron Substitution for Efficient Oxygen Evolution Reaction. Angewandte Chemie, 2018, 130, 2702-2706.	1.6	50
172	Anion–Cation Double Doped Co ₃ O ₄ Microtube Architecture to Promote High-Valence Co Species Formation for Enhanced Oxygen Evolution Reaction. ACS Sustainable Chemistry and Engineering, 2019, 7, 11901-11910.	3.2	50
173	Chitosan Wasteâ€Derived Co and N Coâ€doped Carbon Electrocatalyst for Efficient Oxygen Reduction Reaction. ChemElectroChem, 2015, 2, 1806-1812.	1.7	49
174	Engineering high reversibility and fast kinetics of Bi nanoflakes by surface modulation for ultrastable nickel–bismuth batteries. Chemical Science, 2019, 10, 3602-3607.	3.7	49
175	Porous MoO ₂ nanowires as stable and high-rate negative electrodes for electrochemical capacitors. Chemical Communications, 2017, 53, 3929-3932.	2.2	48
176	<i>Hybrid implanted hybrid</i> hollow nanocube electrocatalyst facilitates efficient hydrogen evolution activity. Journal of Materials Chemistry A, 2019, 7, 11150-11159.	5.2	48
177	Polyhedral Fe ₃ O ₄ nanoparticles for lithium ion storage. New Journal of Chemistry, 2015, 39, 2651-2656.	1.4	46
178	Targeted reversal and phosphorescence lifetime imaging of cancer cell metabolism via a theranostic rhenium(I)-DCA conjugate. Biomaterials, 2018, 176, 94-105.	5.7	46
179	Rational Design of a Ferromagnetic Trinuclear Copper(II) Complex with a Novel in-situ Synthesised Metalloligand. European Journal of Inorganic Chemistry, 2003, 2003, 2385-2388.	1.0	45
180	Monolithic three-dimensional graphene frameworks derived from inexpensive graphite paper as advanced anodes for microbial fuel cells. Journal of Materials Chemistry A, 2016, 4, 6342-6349.	5.2	45

#	Article	IF	CITATIONS
181	Amorphous NiO electrocatalyst overcoated ZnO nanorod photoanodes for enhanced photoelectrochemical performance. New Journal of Chemistry, 2016, 40, 107-112.	1.4	45
182	Ultrahigh energy fiber-shaped supercapacitors based on porous hollow conductive polymer composite fiber electrodes. Journal of Materials Chemistry A, 2018, 6, 12250-12258.	5.2	45
183	TiN Paper for Ultrafast-Charging Supercapacitors. Nano-Micro Letters, 2020, 12, 3.	14.4	44
184	Harnessing hierarchical architectures to trap light for efficient photoelectrochemical cells. Energy and Environmental Science, 2020, 13, 660-684.	15.6	43
185	Facile synthesis of CuO nanorods with abundant adsorbed oxygen concomitant with high surface oxidation states for CO oxidation. RSC Advances, 2012, 2, 11520.	1.7	42
186	Hierarchical Graphene coating for highly sensitive solid phase microextraction of organochlorine pesticides. Talanta, 2016, 160, 217-224.	2.9	42
187	Conductive membranes of EVA filled with carbon black and carbon nanotubes for flexible energy-storage devices. Journal of Materials Chemistry A, 2013, 1, 505-509.	5.2	41
188	Graphene-based metal and nitrogen-doped carbon composites as adsorbents for highly sensitive solid phase microextraction of polycyclic aromatic hydrocarbons. Nanoscale, 2018, 10, 10073-10078.	2.8	41
189	Engineering Heterostructure-Incorporated Metal Silicates Anchored on Carbon Nanotubes for Highly Durable Lithium Storage. ACS Applied Energy Materials, 2021, 4, 1548-1559.	2.5	39
190	Flexible Cellulose Paperâ€based Asymmetrical Thin Film Supercapacitors with Highâ€Performance for Electrochemical Energy Storage. Advanced Functional Materials, 2014, 24, 7093-7101.	7.8	38
191	Three-dimensional Fe3O4 Nanotube Array on Carbon Cloth Prepared from A Facile Route for Lithium ion Batteries. Electrochimica Acta, 2016, 193, 32-38.	2.6	38
192	Oxygenâ€Deficient Threeâ€Đimensional Porous Co ₃ O ₄ Nanowires as an Electrode Material for Water Oxidation and Energy Storage. ChemElectroChem, 2017, 4, 2453-2459.	1.7	38
193	A g-C ₃ N ₄ /WO ₃ photoanode with exceptional ability for photoelectrochemical water splitting. Materials Chemistry Frontiers, 2017, 1, 338-342.	3.2	38
194	Efficient Hydrogen Evolution Electrocatalysis Using Cobalt Nanotubes Decorated with Titanium Dioxide Nanodots. Angewandte Chemie, 2017, 129, 3006-3010.	1.6	37
195	A facile method to produce MoSe2/MXene hybrid nanoflowers with enhanced electrocatalytic activity for hydrogen evolution. Journal of Electroanalytical Chemistry, 2020, 856, 113727.	1.9	37
196	Plasmon-induced carrier separation boosts high-selective photocatalytic CO2 reduction on dagger-axe-like Cu@Co core–shell bimetal. Chemical Engineering Journal, 2021, 417, 129295.	6.6	37
197	ZnO/SnO2 hierarchical and flower-like nanostructures: facile synthesis, formation mechanism, and optical and magnetic properties. CrystEngComm, 2012, 14, 2289.	1.3	36
198	A Robust Versatile Hybrid Electrocatalyst for the Oxygen Reduction Reaction. ACS Applied Materials & Interfaces, 2016, 8, 29356-29364.	4.0	36

#	Article	IF	CITATIONS
199	Porphyrin-based imine gels for enhanced visible-light photocatalytic hydrogen production. Journal of Materials Chemistry A, 2018, 6, 3195-3201.	5.2	36
200	Photo-enhanced Zn–air batteries with simultaneous highly efficient <i>in situ</i> H ₂ O ₂ generation for wastewater treatment. Journal of Materials Chemistry A, 2019, 7, 14129-14135.	5.2	36
201	Silica–Polypyrrole Hybrids as Highâ€Performance Metalâ€Free Electrocatalysts for the Hydrogen Evolution Reaction in Neutral Media. Angewandte Chemie, 2017, 129, 8232-8236.	1.6	35
202	Vertical bismuth oxide nanosheets with enhanced crystallinity: promising stable anodes for rechargeable alkaline batteries. Journal of Materials Chemistry A, 2017, 5, 25539-25544.	5.2	35
203	Improving the Lithiumâ€Storage Properties of Selfâ€Grown Nickel Oxide: A Backâ€Up from TiO ₂ Nanoparticles. ChemElectroChem, 2015, 2, 1243-1248.	1.7	34
204	Nitrogen doped graphene paper as a highly conductive, and light-weight substrate for flexible supercapacitors. RSC Advances, 2014, 4, 51878-51883.	1.7	33
205	Designed synthesis of a porous ultrathin 2D CN@graphene@CN sandwich structure for superior photocatalytic hydrogen evolution under visible light. Chemical Engineering Journal, 2021, 404, 126455.	6.6	32
206	Controllable synthesis of ZnO-based core/shell nanorods and core/shell nanotubes. RSC Advances, 2011, 1, 48.	1.7	31
207	Three-dimensional TiO ₂ /CeO ₂ nanowire composite for efficient formaldehyde oxidation at low temperature. RSC Advances, 2015, 5, 7729-7733.	1.7	31
208	Synthesis, Crystal Structures, and Magnetic Properties of Three New Iron Complexes Derived from 3,5-Bis(pyridin-2-yl)-1,2,4-triazole. Zeitschrift Fur Anorganische Und Allgemeine Chemie, 2006, 632, 475-481.	0.6	30
209	Ni (II) Coordination Supramolecular Grids for Aqueous Nickelâ€Zinc Battery Cathodes. Advanced Functional Materials, 2021, 31, 2100443.	7.8	30
210	Electrochemical synthesis of CoFe2O4 porous nanosheets for visible light driven photoelectrochemical applications. New Journal of Chemistry, 2013, 37, 2965.	1.4	29
211	Porous Hollow Nanorod Arrays Composed of Alternating Pt and Pd Nanocrystals with Superior Electrocatalytic Activity and Durability for Methanol Oxidation. Advanced Materials Interfaces, 2014, 1, 1400005.	1.9	29
212	A recyclable photocatalytic tea-bag-like device model based on ultrathin Bi/C/BiOX (XÂ=ÂCl, Br) nanosheets. Applied Surface Science, 2020, 515, 145967.	3.1	29
213	Acid Treatment Enables Suppression of Electron–Hole Recombination in Hematite for Photoelectrochemical Water Splitting. Angewandte Chemie, 2016, 128, 3464-3468.	1.6	27
214	Surface hydroxylated hematite promotes photoinduced hole transfer for water oxidation. Journal of Materials Chemistry A, 2019, 7, 8050-8054.	5.2	27
215	Assembly of supermolecular complexes with tripodal ligand titmb and tib: a 2D rhombic grid network assembled from 2-connected tib. Dalton Transactions RSC, 2002, , 3886-3891.	2.3	26
216	Etched current collector-guided creation of wrinkles in steel-mesh-supported V ₆ O ₁₃ cathode for lithium-ion batteries. Journal of Materials Chemistry A, 2017, 5, 756-764.	5.2	26

#	Article	IF	CITATIONS
217	A flexible rechargeable quasi-solid-state Ni–Fe battery based on surface engineering exhibits high energy and long durability. Inorganic Chemistry Frontiers, 2018, 5, 1805-1815.	3.0	24
218	Low-valence bicomponent (FeO) _x (MnO) _{1â^'x} nanocrystals embedded in amorphous carbon as high-performance anode materials for lithium storage. Journal of Materials Chemistry A, 2018, 6, 15274-15283.	5.2	24
219	Heterojunction architecture of pTTh nanoflowers with CuOx nanoparticles hybridized for efficient photoelectrocatalytic degradation of organic pollutants. Applied Catalysis B: Environmental, 2020, 277, 119249.	10.8	24
220	Harvesting of Infrared Part of Sunlight to Enhance Polaron Transport and Solar Water Splitting. Advanced Functional Materials, 2022, 32, .	7.8	24
221	Dual doping strategy enhanced the lithium storage properties of graphene oxide binary composites. Journal of Materials Chemistry A, 2016, 4, 13431-13438.	5.2	23
222	Hollow Co2P/Co-carbon-based hybrids for lithium storage with improved pseudocapacitance and water oxidation anodes. Journal of Materials Science and Technology, 2020, 55, 203-211.	5.6	23
223	Novel Fe ₄ -based metal–organic cluster-derived iron oxides/S,N dual-doped carbon hybrids for high-performance lithium storage. Nanoscale, 2021, 13, 716-723.	2.8	23
224	Title is missing!. Transition Metal Chemistry, 2001, 26, 528-531.	0.7	22
225	PtCu alloy nanotube arrays supported on carbon fiber cloth as flexible anodes for direct methanol fuel cell. AICHE Journal, 2016, 62, 975-983.	1.8	22
226	Surface plasmon resonance promoted photoelectrocatalyst by visible light from Au core Pd shell Pt cluster nanoparticles. Electrochimica Acta, 2016, 209, 591-598.	2.6	22
227	Intercalation-type MoP and WP nanodots with abundant phase interface embedded in carbon microflower for enhanced Li storage and reaction kinetics. Electrochimica Acta, 2021, 365, 137354.	2.6	22
228	Controllable electrochemical synthesis of CoFe2O4 nanostructures on FTO substrate and their magnetic properties. New Journal of Chemistry, 2013, 37, 3116.	1.4	21
229	Freeing the Polarons to Facilitate Charge Transport in BiVO ₄ from Oxygen Vacancies with an Oxidative 2D Precursor. Angewandte Chemie, 2019, 131, 19263-19271.	1.6	21
230	Self-sorting multimetal–organic gel electrocatalysts for a highly efficient oxygen evolution reaction. Journal of Materials Chemistry A, 2021, 9, 17451-17458.	5.2	21
231	Earth-abundant metal-free carbon-based electrocatalysts for Zn-air batteries to power electrochemical generation of H2O2 for in-situ wastewater treatment. Chemical Engineering Journal, 2021, 416, 128338.	6.6	21
232	Molten salt synthesis of KCl-preintercalated C3N4 nanosheets with abundant pyridinic-N as a superior anode with 10ÂK cycles in lithium ion battery. Journal of Colloid and Interface Science, 2022, 606, 537-543.	5.0	20
233	Enhanced lithium storage performance of porous exfoliated carbon fibers <i>via</i> anchored nickel nanoparticles. RSC Advances, 2018, 8, 17056-17059.	1.7	19
234	Surface functionalized 3D carbon fiber boosts the lithium storage behaviour of transition metal oxide nanowires <i>via</i> strong electronic interaction and tunable adsorption energy. Nanoscale Horizons, 2019, 4, 1402-1410.	4.1	19

#	Article	IF	CITATIONS
235	Integrating boron atoms into ultrathin organic polymer for visible light photocatalytic CO ₂ reduction to CH ₄ with nearly 100% selectivity. Journal of Materials Chemistry A, 2022, 10, 5287-5294.	5.2	19
236	BiOI Nanopaper As a High-Capacity, Long-Life and Insertion-Type Anode for a Flexible Quasi-Solid-State Zn-Ion Battery. ACS Applied Materials & Interfaces, 2022, 14, 25516-25523.	4.0	19
237	Controllable growth of La(OH)3 nanorod and nanotube arrays. CrystEngComm, 2010, 12, 4066.	1.3	18
238	General electrochemical assembling to porous nanowires with high adaptability to water treatment. CrystEngComm, 2011, 13, 2451.	1.3	18
239	Strategy for stabilizing noble metal nanoparticles without sacrificing active sites. Chemical Communications, 2019, 55, 6846-6849.	2.2	18
240	Lanthanide-Based Dual Modulation in Hematite Nanospindles for Enhancing the Photocatalytic Performance. ACS Applied Nano Materials, 2022, 5, 8557-8565.	2.4	18
241	Anion-controlled Formation of Silver(I) Complexes of A Hexaazamacrocyclic Schiff Base: Synthesis, Structures and Electrochemistry. Supramolecular Chemistry, 1999, 11, 119-133.	1.5	17
242	Mild metal-organic-gel route for synthesis of stable sub-5-nm metal-organic framework nanocrystals. Nano Research, 2017, 10, 3621-3628.	5.8	17
243	Fast synthesis of porous iron doped CeO2 with oxygen vacancy for effective CO2 photoreduction. Journal of Colloid and Interface Science, 2022, 608, 1792-1801.	5.0	17
244	Tailoring superficial morphology, defect and functional group of commercial carbon cloth for a flexible, stable and high-capacity anode in sodium ion battery. Electrochimica Acta, 2021, 374, 137934.	2.6	16
245	3D V ₃ O ₇ ·H ₂ O/Partially Exfoliated Carbon Nanotube Composites with Significantly Improved Lithium Storage Ability. Particle and Particle Systems Characterization, 2016, 33, 531-537.	1.2	15
246	Using pulverization phenomenon to extend electrodes cyclic life of ternary metal oxides. Materials Today Energy, 2018, 9, 311-318.	2.5	15
247	Hydrogen bond induced change of geometry and crystallized form of copper(II) complexes: syntheses and crystal structure of complexes with Schiff-base ligands containing two imidazolyl groups. Dalton Transactions RSC, 2001, , 845-849.	2.3	14
248	Enhanced Photoelectrochemical Oxygen Evolution Reaction Ability of Ironâ€Derived Hematite Photoanode with Titanium Modification. Chemistry - A European Journal, 2015, 21, 19250-19256.	1.7	14
249	Enhanced Photoelectrochemical Activity by Autologous Cd/CdO/CdS Heterojunction Photoanodes with High Conductivity and Separation Efficiency. Chemistry - A European Journal, 2017, 23, 9625-9631.	1.7	14
250	3D Hierarchical Nanorod@Nanobowl Array Photoanode with a Tunable Lightâ€Trapping Cutoff and Bottomâ€Selective Field Enhancement for Efficient Solar Water Splitting. Small, 2019, 15, e1804976.	5.2	14
251	Controllable synthesis of porous silver cyanamide nanocrystals with tunable morphologies for selective photocatalytic CO2 reduction into CH4. Journal of Colloid and Interface Science, 2021, 593, 152-161.	5.0	14
252	Turning commercial MnO2 (≥85Âwt%) into high-crystallized K+-doped LiMn2O4 cathode with superior structural stability by a low-temperature molten salt method. Journal of Colloid and Interface Science, 2022, 608, 1377-1383.	5.0	14

#	Article	IF	CITATIONS
253	A Simple and Highly Sensitive Thymine Sensor for Mercury Ion Detection Based on Surface Enhanced Raman Spectroscopy and the Mechanism Study. Nanomaterials, 2017, 7, 192.	1.9	13
254	Covalently Modified Electrode with Pt Nanoparticles Encapsulated in Porous Organic Polymer for Efficient Electrocatalysis. ACS Applied Nano Materials, 2018, 1, 6477-6482.	2.4	13
255	Phytic Acidâ€Based FeCo Bimetallic Metalâ€Organic Gels for Electrocatalytic Oxygen Evolution Reaction. Chemistry - an Asian Journal, 2021, 16, 3213-3220.	1.7	13
256	Synthesis of Ceâ^'Fe Intermetallic Compounds with Foam Structures via Electrochemical Deposition. Chemistry of Materials, 2007, 19, 2283-2287.	3.2	12
257	Toward Efficient Charge Collection and Light Absorption: A Perspective of Light Trapping for Advanced Photoelectrodes. Journal of Physical Chemistry C, 2019, 123, 18753-18770.	1.5	12
258	Defect Engineering Enhances the Charge Separation of CeO2 Nanorods toward Photocatalytic Methyl Blue Oxidation. Nanomaterials, 2020, 10, 2307.	1.9	12
259	Electrochemical Activation of Heterometallic Nanofibers for Hydrogen Evolution. ACS Applied Nano Materials, 2020, 3, 2393-2401.	2.4	12
260	Imine Gels Based on Ferrocene and Porphyrin and Their Electrocatalytic Property. Chemistry - an Asian Journal, 2020, 15, 1963-1969.	1.7	12
261	Co ₃ O ₄ @Co Nanoparticles Embedded Porous Nâ€Rich Carbon Matrix for Efficient Oxygen Reduction. Particle and Particle Systems Characterization, 2017, 34, 1700074.	1.2	11
262	Enhanced catalytic activity of Au core Pd shell Pt cluster trimetallic nanorods for CO ₂ reduction. RSC Advances, 2019, 9, 10168-10173.	1.7	11
263	In Situ Monitoring Small Energy Storage Change of Electrochromic Supercapacitors via Perovskite Photodetectors. Small Methods, 2020, 4, 1900731.	4.6	11
264	Construction of cobalt vacancies in cobalt telluride to induce fast ionic/electronic diffusion kinetics for lithium-ion half/full batteries. Journal of Materials Science and Technology, 2022, 127, 124-132.	5.6	11
265	A general method to synthesize metal/N-doped carbon nanocomposites with advanced sodium storage properties. Journal of Alloys and Compounds, 2021, 858, 157686.	2.8	10
266	Boosting the Photoelectrochemical Water Oxidation at Hematite Photoanode by Innovating a Hierarchical Ball-on-Wire-Array Structure. ACS Applied Energy Materials, 2018, 1, 5836-5841.	2.5	9
267	SnS/SnO heterostructures embedded in porous carbon microcages by boosting charge transfer for enhanced sodium-ion storage. Materials Technology, 2018, 33, 548-554.	1.5	9
268	Syntheses, Crystal Structures, Superoxide Dismutase-Like Behaviors and Physical Properties of Four Manganese(III) Complexes with Di-Schiff Bases Derived from Salicylaldehyde and Polyamines. Journal of Coordination Chemistry, 2002, 55, 843-852.	0.8	8
269	Electrochemical preparation and magnetic properties of submicron Co x Pb1â^'x dendrites. Journal of Solid State Electrochemistry, 2011, 15, 1193-1199.	1.2	8
270	Lithium Ferrites@Polydopamine Core–Shell Nanoparticles as a New Robust Negative Electrode for Advanced Asymmetric Supercapacitors. Particle and Particle Systems Characterization, 2018, 35, 1800128.	1.2	8

#	Article	IF	CITATIONS
271	Title is missing!. Transition Metal Chemistry, 1999, 24, 49-51.	0.7	7
272	Promoting Alternative Flexible Substrate for Electrode Materials to Achieve Enhanced Lithium Storage Properties. ChemistrySelect, 2018, 3, 6965-6971.	0.7	7
273	Multifunctional carbon-confined FeS nanoparticles for a self-supporting and high-capacity cathode in lithium ion battery. Journal of Electroanalytical Chemistry, 2021, 880, 114849.	1.9	7
274	One-Step Synthesis of ZnNCN Nanoparticles with Adjustable Composition for an Advanced Anode in Lithium Ion Battery. ACS Applied Energy Materials, 2021, 4, 4290-4296.	2.5	7
275	Line defects in plasmatic hollow copper ball boost excellent photocatalytic reaction with pure water under ultra-low CO2 concentration. Journal of Colloid and Interface Science, 2021, 603, 530-538.	5.0	7
276	Reaction of sulfur-containing structural units of transition metals. Science in China Series B: Chemistry, 1997, 40, 634-642.	0.8	6
277	Efficient electroless nickel plating from highly active Ni–B nanoparticles for electric circuit patterns on Al2O3 ceramics. Journal of Materials Chemistry C, 2013, 1, 5149.	2.7	6
278	Enhanced Photocatalytic Activity from Mixtureâ€Fuel Cells by ZnO Templateâ€Assisted Pdâ€Pt Hollow Nanorods. ChemistrySelect, 2017, 2, 9842-9846.	0.7	6
279	Zrâ€Based Metalâ€Organic Framework Films Grown on Bioâ€Template for Photoelectrocatalysis. ChemistrySelect, 2020, 5, 13855-13861.	0.7	6
280	Structural, Photocatalytic and Enhanced Magnetic Properties of Bi1-xHoxFeO3Nanoparticles Synthesized Via Sol-Gel Method. Ferroelectrics, 2015, 489, 65-72.	0.3	5
281	CO ₂ Electroreduction: Intermediates Adsorption Engineering of CO ₂ Electroreduction Reaction in Highly Selective Heterostructure Cuâ€Based Electrocatalysts for CO Production (Adv. Energy Mater. 27/2019). Advanced Energy Materials, 2019, 9, 1970107.	10.2	5
282	Title is missing!. Journal of Chemical Crystallography, 1999, 29, 409-412.	0.5	4
283	Title is missing!. Journal of Cluster Science, 1999, 10, 429-443.	1.7	4
284	Enhancing Catalytic Activity and Selectivity by Plasmon-Induced Hot Carriers. IScience, 2020, 23, 101107.	1.9	4
285	Tailoring hydrophily and composition of BiOI for an ultrafast photodegradation of tetracycline hydrochloride. Journal of Environmental Chemical Engineering, 2021, 9, 106292.	3.3	4
286	Investigating Why Sulfurization Can Greatly Improve Ethanol Selectivity for Carbon Dioxide Electroreduction. CCS Chemistry, 2022, 4, 3319-3328.	4.6	3
287	Crystal structure of [Co(o-SC6H4NH2){P(OMe)3}3]PF6. Journal of Chemical Crystallography, 1998, 28, 635-638.	0.5	2
288	Synthesis, Crystal Structure and Electrochemical Behavior of a Fe(II) Complex of 8â€Mercaptoquinoline (Hmtq) with Trimethylphosphite Participation. Journal of the Chinese Chemical Society, 1999, 46, 159-163.	0.8	2

#	Article	IF	CITATIONS
289	Electrolyte additive strategy enhancing the electrochemical performance of a soft-packed LiCoO ₂ //graphite full cell. Dalton Transactions, 2022, 51, 8723-8732.	1.6	2
290	PREPARATION, CRYSTAL STRUCTURE AND PROPERTIES OF [{MnL(PHEN)2}(ClO4)·1.25H2O]n[HL =N-(1-CARBOXYPROPIONYL)AMINOPYRIDINE; PHEN =O-PHENANTHROLINE]. Journal of Coordination Chemistry, 1998, 46, 105-114.	0.8	1
291	Synthesis and crystal structure of [Co(mpt)2{P(OCH3)3}2]BF4 (Hmpt = 2-mercaptothiazoline). Chinese Journal of Chemistry, 2010, 17, 36-41.	2.6	1
292	Synthesis and crystal structure of a phosphite nickel(II) 8-mercaptoquinoline complex. Transition Metal Chemistry, 1999, 24, 274-276.	0.7	0
293	Frontispiece: Boosting the Energy Density of Carbonâ€Based Aqueous Supercapacitors by Optimizing the Surface Charge. Angewandte Chemie - International Edition, 2017, 56, .	7.2	0
294	Frontispiz: Boosting the Energy Density of Carbonâ€Based Aqueous Supercapacitors by Optimizing the Surface Charge. Angewandte Chemie, 2017, 129, .	1.6	0
295	Frontispiece: Designing Carbon Based Supercapacitors with High Energy Density: A Summary of Recent Progress. Chemistry - A European Journal, 2018, 24, .	1.7	0
296	Water Splitting: 3D Hierarchical Nanorod@Nanobowl Array Photoanode with a Tunable Lightâ€Trapping Cutoff and Bottomâ€Selective Field Enhancement for Efficient Solar Water Splitting (Small 14/2019). Small, 2019, 15, 1970074.	5.2	0